A Novel Deblocking Quantization Table for Luminance Component in Baseline JPEG

Qiming Fu, Baochen Jiang, Chengyou Wang, and Xiao Zhou
School of Mechanical, Electrical and Information Engineering, Shandong University, Weihai 264209, China
Email: fqmsdu@163.com; {jbc, wangchengyou, zhouxiao}@sdu.edu.cn

Abstract —All Phase Biorthogonal Transform (APBT), a DCT-like transform generated from All Phase Digital Filter (APDF), can be used in baseline JPEG by replacing conventional Discrete Cosine Transform (DCT), and the image compression scheme is called APBT-based JPEG (APBT-JPEG). APBT-JPEG can achieve better coding performance but at the expense of an increased computational complexity, because there is no fast algorithm for computing APBT. With our in-depth study on APBT-JPEG, we have found the relation between APBT-JPEG and DCT-JPEG (baseline JPEG) in this paper. In order to avoid extra computational complexity in APBT-JPEG, we propose a novel quantization table used in DCT-JPEG and an almost identical coding performance is achieved compared with APBT-JPEG. Tested by natural images, experimental results show that compared with other quantization tables, at low bit rates in DCT-JPEG, the performance both in terms of PSNR and visual quality can be improved by using our proposed quantization table, and the blocking artifacts in reconstructed image have been reduced significantly. For these reasons, we can foresee that the proposed quantization table will be widely used in the future.

Index Terms—Image compression, deblocking, quantization table, All Phase Biorthogonal Transform (APBT), Discrete Cosine Transform (DCT), JPEG

I. Introduction

In spite of the rapid development of huge capacity and high speed storage devices, lossy compression techniques of multimedia data, and especially images, are still increasingly used. Compared with the emerging wavelet-based standard JPEG2000 [1] and the latest LBT-based standard JPEG-XR [2], the DCT-based JPEG standard [3] known as the baseline JPEG remains to be the most commonly employed lossy compression algorithm for still images due to its high effectiveness and low computational complexity. However, DCT-based JPEG image compression method suffers from some annoying blocking artifacts at low bit rates, which results in visible discontinuities across block boundaries [4]. This is mainly due to independent processing of blocks in DCT-based JPEG.

Therefore, many kinds of post-filtering techniques [5], [6] for deblocking artifacts are proposed, which reduce the visibility of blocking artifacts in reconstructed image but increase complexity of the decoding process. Interestingly, unlike post-filtering techniques, a new kind of JPEG-like image compression scheme without any deblocking technique called All Phase Biorthogonal Transform (APBT)-based JPEG was proposed, of which blocking artifacts in reconstructed image have been reduced significantly [7]. In the following, we focus on the relevant advances in APBT-based image/video compression scheme.

In the light of all phase digital filter (APDF) theory [8], three kinds of APBTs based on the Walsh-Hadamard Transform (WHT), the discrete cosine transform (DCT) and the Inverse Discrete Cosine Transform (IDCT) were proposed [7]. These APBTs could be used in baseline JPEG by replacing conventional DCT; so an image compression scheme called APBT-JPEG was generated. In fact, among these APBTs, APBT based on IDCT always achieves best coding performance in image compression. For this reason, in this paper our research work focuses on APBT based on IDCT (called APBT in this paper).

Compared with DCT-JPEG using quantization table suggested by JPEG (called default quantization table in this paper), better coding performance was produced in APBT-JPEG at various bit rates. Actually, the merits of APBT-JPEG are less blocking artifacts in reconstructed image and simple uniform quantization table in quantization procedure, but its shortcoming is that there is no fast APBT algorithm, which brings extra burden on complexity to perform APBT-JPEG.

Due to some superiority of APBT-JPEG, its theory and application have been researched further in recent years. APBT was applied to color image compression instead of DCT [9], the blocking artifacts in reconstructed image have been reduced significantly and better performance is achieved at various bit rates. Moreover, with directional DCT and shape-adaptive DCT used for reference, directional APBT (D-APBT) [10] and shape-adaptive APBT (SA-APBT) [11] were proposed and better performance is achieved in image coding application. APBT also has been used in MPEG-4 video compression [12] instead of DCT, approximate performance is obtained. However, in image/video compression, since DCT has been widely used and there are many efficient

Manuscript received April 30, 2015; revised August 19, 2015.
This work was supported by the National Natural Science Foundation of China under Grant No. 61201371 and the promotive research fund for excellent young and middle-aged scientists of Shandong Province, China under Grant No. BS2013DX022.
Corresponding author email: jbc@sdu.edu.cn.
doi:10.12720/jcm.10.8.629-637.

algorithms for its fast computation [13], [14], the popularization of APBT seems to be difficult.

Note that the default quantization table is not a part of the JPEG standard. The JPEG baseline codec allows users themselves to redefine the quantization table to control the compression ratio and the quality of the reconstructed image. Therefore, by finding the relation between DCT-JPEG and APBT-JPEG, we devote ourselves to seeking a novel quantization table in DCT-JPEG, which can achieve identical coding performance compared with APBT-JPEG, and we hope our proposed quantization table will be widely used in the future.

The rest of this paper is organized as follows. In Section II, the relationship between DCT-JPEG and APBT-JPEG is revealed and a quantization table $\boldsymbol{Q}^*$ is found, which acts as a bridge between these two different image compression schemes. Based on quantization table $\boldsymbol{Q}^*$, in order to get an approximate quantization table which remains faithful to the baseline JPEG syntax, the corresponding algorithm and procedure are presented in Section III. In comparison with APBT-JPEG using uniform quantization table and DCT-JPEG using different quantization tables (including proposed quantization table), corresponding experimental simulating is done, and both objective and subjective quality assessment results of reconstructed images are presented in Section IV. Finally, conclusions and discussions for further research are given in Section V.

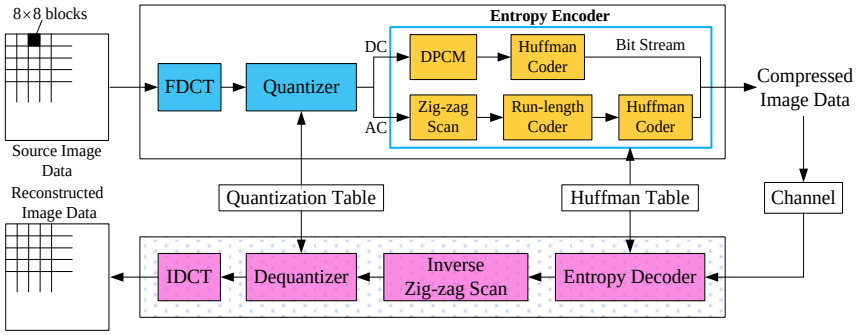

Fig. 1. The scheme of DCT-JPEG (baseline JPEG) image codec. The compression itself is performed in four sequential steps: DCT computation, quantization, zig-zag scan and entropy coding.

II. Relation between APBT-JPEG and DCT-JPEG

A. DCT-Based JPEG Image Compression Scheme

The scheme of DCT-JPEG (baseline JPEG) image codec can be seen in Fig. 1.

The encoder of DCT-JPEG is mainly composed of four parts: forward discrete cosine transform (FDCT), quantization, zig-zag scan, and entropy encoder. In the encoding process, the input image is grouped into blocks of size 8×8. Prior to computing the FDCT, the input image data are level shifted to a signed two's complement representation. For 8-bit input precision, the level shift is achieved by subtracting 128. And then, each block is transformed by the FDCT into 64 DCT coefficients, the DC coefficient and the 63 AC coefficients. After quantization, the DC coefficient of each block is coded in a differential pulse code modulation (DPCM), and then is coded using Huffman coding. The 63 quantized AC coefficients are converted into a 1-D zig-zag sequence, preparing for entropy encoding (run-length coding and followed by Huffman coding).

The decoder also contains four major parts: entropy decoder, inverse zig-zag scan, dequantization, and IDCT, which performs essentially the inverse of its corresponding main procedure within the encoder.

In DCT-JPEG's forward transform, the conventional 2-D DCT is always implemented separately by two 1-D DCTs. Let us use $\boldsymbol{X}$ and $\boldsymbol{C}$ to denote an image block and the DCT matrix with size of $N\times N$, respectively. After the conventional 2-D DCT, the transform coefficient block $\boldsymbol{Y}$ can be expressed as $\boldsymbol{Y}=\boldsymbol{C}\boldsymbol{X}\boldsymbol{C}^{\mathrm{T}}$, where $\boldsymbol{C}^{\mathrm{T}}$ is the transpose matrix of $\boldsymbol{C}$,

$$C(i,j)=\begin{cases}\sqrt{\dfrac{1}{N}}, & i=0,\ j=0,1,\cdots,N-1,\\ \sqrt{\dfrac{2}{N}}\cos\dfrac{i(2j+1)\pi}{2N}, & i=1,2,\cdots,N-1,\\ & j=0,1,\cdots,N-1.\end{cases} \tag{1}$$

The quantizer in DCT-JPEG is defined by the following equation. Rounding is to the nearest integer:

$$Y_Q(u,v)=\mathrm{round}\left(\frac{Y(u,v)}{c\times Q(u,v)}\right) \tag{2}$$

where $Y(u,v)$ is an element of $\boldsymbol{Y}$; $Q(u,v)$, an element of quantization table $\boldsymbol{Q}$, is the corresponding quantization step size, and $Y_Q(u,v)$ is the quantized transform coefficient, normalized by the quantization step size; c is a constant factor called quantization factor here. Quantization factor which is chosen to satisfy rate and quality control criteria is an important parameter in bit rate control here.

At the dequantizer in decoder, this normalization is removed by the following equation, which defines dequantization:

$$\tilde{Y}(u,v)=Y_Q(u,v)\times[c\times Q(u,v)] \tag{3}$$

where $\tilde{Y}(u,v)$ is the output of dequantizer, and it is an element of dequantized transform coefficient block $\tilde{\boldsymbol{Y}}$.

Since DCT is an orthogonal transform, we can use $\tilde{\boldsymbol{X}} = (\boldsymbol{C}^{-1})\tilde{\boldsymbol{Y}}(\boldsymbol{C}^{-1})^{\mathrm{T}} = \boldsymbol{C}^{\mathrm{T}}\tilde{\boldsymbol{Y}}\boldsymbol{C}$ to reconstruct the image.

B. Relation between APBT and DCT

In the design of APDF based on IDCT, there is a transition matrix $\boldsymbol{V}$ which connects IDCT domain and time domain, and we call it APBT [7]. APBT was found by chance. It is proved to be a high efficient transform method of signal representation and has been applied successfully in image/video coding. The elements in the APBT matrix $\boldsymbol{V}$ are:

$$V(i,j) = \begin{cases} \dfrac{1}{N}, & i = 0, j = 0,1,\cdots,N-1, \\ \dfrac{N-i+\sqrt{2}-1}{N^2}\cos\dfrac{i(2j+1)\pi}{2N}, & i = 1,2,\cdots,N-1, \\ & j = 0,1,\cdots,N-1. \end{cases} \tag{4}$$

The IAPBT matrix $\boldsymbol{V}^{-1}$ can be formulated as:

$$V^{-1}(i,j) = \begin{cases} 1, & j = 0, i = 0,1,\cdots,N-1, \\ \dfrac{2N}{N-j+\sqrt{2}-1}\cos\dfrac{j(2i+1)\pi}{2N}, & j = 1,2,\cdots,N-1, \\ & i = 0,1,\cdots,N-1. \end{cases} \tag{5}$$

For 1-D vector $\boldsymbol{x}$, we define the APBT as $\boldsymbol{y} = \boldsymbol{V}\boldsymbol{x}$ and the inverse APBT (IAPBT) $\boldsymbol{x} = \boldsymbol{V}^{-1}\boldsymbol{y}$. We define the 2-D APBT as $\boldsymbol{Y} = \boldsymbol{V}\boldsymbol{X}\boldsymbol{V}^{\mathrm{T}}$ and the IAPBT is $\boldsymbol{X} = (\boldsymbol{V}^{-1})\boldsymbol{Y}(\boldsymbol{V}^{-1})^{\mathrm{T}}$, where $\boldsymbol{X}$ denotes an image matrix, $\boldsymbol{Y}$ denotes the corresponding matrix of transform coefficients.

According to Eq. (1) and Eq. (4), the relation between APBT and DCT can be summarized as:

$$\begin{cases} \boldsymbol{V} = \boldsymbol{D}\boldsymbol{C}, \\ \boldsymbol{V}^{-1} = \boldsymbol{C}^{\mathrm{T}}\boldsymbol{D}^{-1}. \end{cases} \tag{6}$$

where $\boldsymbol{V}$ denotes the APBT matrix and $\boldsymbol{C}$ denotes the DCT matrix. $\boldsymbol{D}$ is a diagonal matrix, and the diagonal elements of it are given by:

$$D(n,n) = \begin{cases} \dfrac{1}{\sqrt{N}}, & n = 0, \\ \dfrac{1}{N\sqrt{N}}\left(1+\dfrac{N-n-1}{\sqrt{2}}\right), & n = 1,2,\cdots,N-1. \end{cases} \tag{7}$$

$\boldsymbol{D}^{-1}$, the inverse matrix of $\boldsymbol{D}$, is also a diagonal matrix and the diagonal elements of it are given by:

$$D^{-1}(n,n) = \begin{cases} \sqrt{N}, & n = 0, \\ \dfrac{N\sqrt{2N}}{N-n+\sqrt{2}-1}, & n = 1,2,\cdots,N-1. \end{cases} \tag{8}$$

APBT, which is considered to be a DCT-like transform, is non-orthogonal, but the development of the fast algorithm for computing APBT is not impossible. However, to the best of our knowledge, it is a pity that there is no fast algorithm for computing APBT. Thus, with APBT replacing DCT in APBT-JPEG at present, higher computational complexity is required during transform procedure.

C. Relation between APBT-JPEG and DCT-JPEG

In this subsection, we study the relation between APBT-JPEG and DCT-JPEG.

The scheme of APBT-JPEG image codec is shown in Fig. 2. The basic processes are similar to the DCT-JPEG algorithm. The differences between them are the transform (DCT or APBT) and quantizer (quantization table or uniform quantization table). Other steps of APBT-JPEG algorithm are identical to DCT-based JPEG. The quantization tables used in APBT-JPEG and DCT-JPEG are shown respectively in Fig. 3.

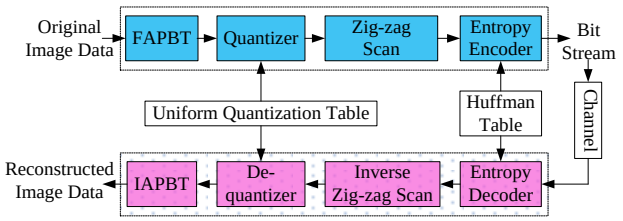

Fig. 2. The scheme of APBT-JPEG image codec. The differences between DCT-JPEG and APBT-JPEG are the transform and quantization table. Other steps of APBT-JPEG scheme are identical to DCT-based JPEG.

As [7] tells us, in APBT-JPEG scheme, due to adopting uniform quantization table and saving the memory space of the quantization table, when adjusting the bit rates, each image block can save 63 multiplication operations between quantization factor and quantization table. This is a good aspect of APBT-JPEG scheme.

1	1	1	1	1	1	1	1
1	1	1	1	1	1	1	1
1	1	1	1	1	1	1	1
1	1	1	1	1	1	1	1
1	1	1	1	1	1	1	1
1	1	1	1	1	1	1	1
1	1	1	1	1	1	1	1
1	1	1	1	1	1	1	1

(a)

16	11	10	16	24	40	51	61
12	12	14	19	26	58	60	55
14	13	16	24	40	57	69	56
14	17	22	29	51	87	80	62
18	22	37	56	68	109	103	77
24	35	55	64	81	104	113	92
49	64	78	87	103	121	120	101
72	92	95	98	112	100	103	99

(b)

Fig. 3. The quantization tables: (a) Uniform quantization table used in APBT-JPEG, and (b) Quantization table suggested by JPEG used in DCT-JPEG.

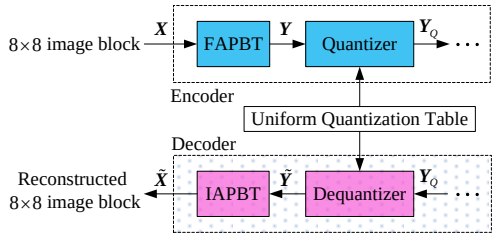

Fig. 4. Transform (inverse transform) and quantization (dequantization) in APBT-JPEG.

As Fig. 4 shows, we define the 2-D APBT as $\boldsymbol{Y} = \boldsymbol{V}\boldsymbol{X}\boldsymbol{V}^{\mathrm{T}}$ and the IAPBT is $\tilde{\boldsymbol{X}} = (\boldsymbol{V}^{-1})\tilde{\boldsymbol{Y}}(\boldsymbol{V}^{-1})^{\mathrm{T}}$, where $\boldsymbol{X}$ denotes an 8×8 image block, $\boldsymbol{Y}$ denotes the corresponding block matrix in the transform domain,

which is the input of the quantizer, and $\tilde{\boldsymbol{X}}$ denotes a reconstructed 8×8 image block, $\tilde{\boldsymbol{Y}}$ denotes the corresponding block matrix in the transform domain, which is the output of the dequantizer.

Then, the forward transformation operations in APBT-JPEG can be performed using the APBT transform as:

$$\begin{aligned}\boldsymbol{Y} &= \boldsymbol{V}\boldsymbol{X}\boldsymbol{V}^{\mathrm{T}} = (\boldsymbol{D}\boldsymbol{C})\boldsymbol{X}(\boldsymbol{D}\boldsymbol{C})^{\mathrm{T}} \\ &= \boldsymbol{D}\boldsymbol{C}\boldsymbol{X}\boldsymbol{C}^{\mathrm{T}}\boldsymbol{D}^{\mathrm{T}} = \boldsymbol{D}(\boldsymbol{C}\boldsymbol{X}\boldsymbol{C}^{\mathrm{T}})\boldsymbol{D}\end{aligned} \tag{9}$$

The inverse transformation operations in APBT-JPEG can be performed using the APBT transform as:

$$\begin{aligned}\tilde{\boldsymbol{X}} &= (\boldsymbol{V}^{-1})\tilde{\boldsymbol{Y}}(\boldsymbol{V}^{-1})^{\mathrm{T}} = (\boldsymbol{C}^{\mathrm{T}}\boldsymbol{D}^{-1})\tilde{\boldsymbol{Y}}(\boldsymbol{C}^{\mathrm{T}}\boldsymbol{D}^{-1})^{\mathrm{T}} \\ &= \boldsymbol{C}^{\mathrm{T}}\boldsymbol{D}^{-1}\tilde{\boldsymbol{Y}}(\boldsymbol{D}^{-1})^{\mathrm{T}}\boldsymbol{C} = \boldsymbol{C}^{\mathrm{T}}(\boldsymbol{D}^{-1}\tilde{\boldsymbol{Y}}\boldsymbol{D}^{-1})\boldsymbol{C}\end{aligned} \tag{10}$$

Since the quantization (dequantization) is applied on the block matrix in the transform domain, according to Eq. (9) and Eq. (10), the diagonal matrix $\boldsymbol{D}$ ($\boldsymbol{D}^{-1}$) can be merged into the quantization (dequantization) matrix. Such a merging is also suggested in many papers, including [15]. In APBT-JPEG, since the diagonal matrix $\boldsymbol{D}$ ($\boldsymbol{D}^{-1}$) in transform (inverse transform) procedure is merged into the quantization (dequantization) matrix, original uniform quantization table is changed into a new quantization table and the APBT degenerates into DCT. Therefore, the APBT-JPEG can be implemented by DCT-JPEG with a different quantization table called $\boldsymbol{Q}^*$ in this paper. The elements in $\boldsymbol{Q}^*$ are formulated as:

$$Q^*(u,v) = D^{-1}(u,u)D^{-1}(v,v) \tag{11}$$

where $u = 0,1,\cdots,N-1$, and $v = 0,1,\cdots,N-1$.

For 8×8 image block matrices in JPEG, the variable N in Eq. (11) is equal to the value 8, and corresponding quantization table $\boldsymbol{Q}^*$ calculated by Eq. (11) is shown in Fig. 5. Compared with APBT-JPEG, an identical coding performance would be achieved by using DCT-JPEG with the quantization table $\boldsymbol{Q}^*$ instead of the default quantization table suggested by JPEG. Corresponding verification experiment will be done and the results will be presented in Section IV. The relationship between APBT-JPEG and DCT-JPEG is illustrated in Fig. 6.

8.0000	12.2076	14.1108	16.7170	20.5041	26.5097	37.4903	64.0000
12.2076	18.6282	21.5324	25.5094	31.2883	40.4524	57.2083	97.6607
14.1108	21.5324	24.8893	29.4864	36.1662	46.7591	66.1273	112.8864
16.7170	25.5094	29.4864	34.9325	42.8461	55.3954	78.3410	133.7364
20.5041	31.2883	36.1662	42.8461	52.5525	67.9448	96.0884	164.0331
26.5097	40.4524	46.7591	55.3954	67.9448	87.8453	124.2320	212.0773
37.4903	57.2083	66.1273	78.3410	96.0884	124.2320	175.6906	299.9227
64.0000	97.6607	112.8864	133.7364	164.0331	212.0773	299.9227	512.0000

Fig. 5. Luminance quantization table $\boldsymbol{Q}^*$ calculated by Eq. (11) ($N=8$), which acts as a bridge between DCT-JPEG and APBT-JPEG.

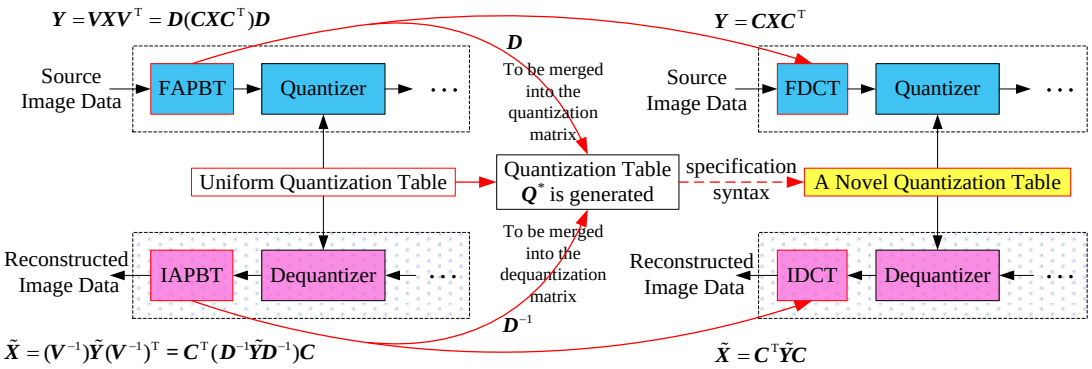

Fig. 6. Procedure of obtaining the proposed quantization table, and description to the relationship between APBT-JPEG and DCT-JPEG.

III. Deblocking Quantization Table Used in Baseline JPEG

A. Generalized Pattern Search Algorithm (GPSA)

Before presenting the procedure of looking for the proposed quantization table, it is worth introducing some related issues such as optimization technique which will be used in following subsection.

Unconstrained optimization problem can be formulated as a *D*-dimensional minimization problem as follows:

$$\min_{\boldsymbol{x}} f(\boldsymbol{x}),\ \boldsymbol{x} = [x_1, x_2, \cdots, x_D]^{\mathrm{T}} \tag{12}$$

where f is the objective function and parameters vector $\boldsymbol{x}$ is considered to be a point in the *D*-dimensional real space $\boldsymbol{R}^D$.

There is a relatively conventional optimization technique called generalized pattern search algorithm (GPSA), which is a typical direct search method [16], [17]. GPSA is an iterative method that generates a sequence of feasible iterates whose objective function

value is non-increasing. At any given iteration, the objective function is evaluated at a finite number of points on a mesh in order to try to find one that yields a decrease in the objective function value. Each iteration is divided into two phases: an optional search and a local poll [18]. A flow chart of generalized pattern search algorithm is shown in Fig. 7.

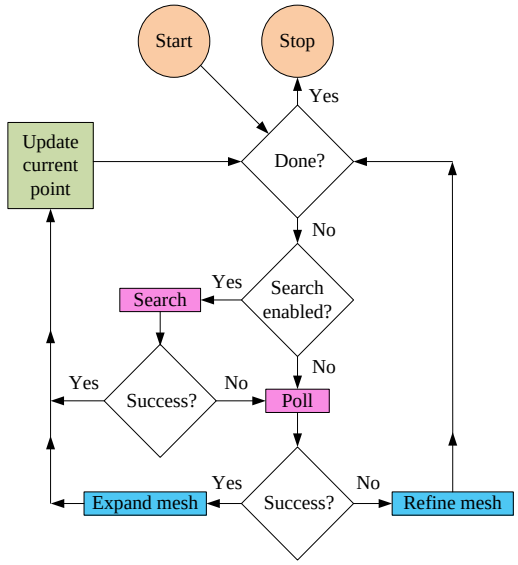

Fig. 7. The flow chart of generalized pattern search algorithm.

GPSA is an optimization technique that does not require gradient information of the objective function. And it is based on a simple concept that is easy to be implemented and is efficient when computed. Simulating in MATLAB, we can call MATLAB function called "pattern search" to implement GPSA for convenience.

B. *The Algorithm to Obtain Deblocking Quantization Table Used in Baseline JPEG*

In baseline JPEG, the precision of the quantization table $\boldsymbol{Q}$ values is specified to 8-bit, which indicates the range of quantization step size is 1~255. For this reason, $\boldsymbol{Q}^*$ cannot be used directly in baseline JPEG. In order to remain faithful to the baseline JPEG syntax, we shall look for an integer (1~255) quantization table $\boldsymbol{Q}^{int}$, which is the most robust approximation of $\boldsymbol{Q}^*$. In what follows, we will present how to obtain $\boldsymbol{Q}^{int}$ from $\boldsymbol{Q}^*$.

$$Q^s(u,v)=\frac{Q^*(u,v)}{\lambda},\quad \frac{512}{255}\le\lambda\le 16 \tag{13}$$

where parameter λ is defined as quantization table scale factor here which can be merged into the quantization factor c in baseline JPEG. From Fig. 5, it is easy to see that the range of $\boldsymbol{Q}^*$ values is from 8 to 512. After $\boldsymbol{Q}^*$ has been scaled by parameter λ in Eq. (13), $\boldsymbol{Q}^s$ is obtained and the range of $\boldsymbol{Q}^s$ values is from 0.5 to 255.

$$Q^{int}(u,v)=\text{round}\,[Q^s(u,v)] \tag{14}$$

In Eq. (14), $\boldsymbol{Q}^{int}$ is yielded where each element is an integer with a range of 1 to 255. Thus, $\boldsymbol{Q}^{int}$ can be used directly in baseline JPEG. The difference between $\boldsymbol{Q}^{int}$ and $\boldsymbol{Q}^s$ is measured by mean absolute percentage error (MAPE). The MAPE between $\boldsymbol{Q}^{int}$ and $\boldsymbol{Q}^s$ is defined as Eq. (15). The smaller the MAPE between $\boldsymbol{Q}^{int}$ and $\boldsymbol{Q}^s$, the better approximation is achieved.

$$\text{MAPE}=\frac{1}{8\times 8}\sum_{u=0}^{7}\sum_{v=0}^{7}\left|\frac{Q^{int}(u,v)}{Q^s(u,v)}-1\right| \tag{15}$$

In this paper, we aim to look for an integer quantization table which is the most robust approximation of $\boldsymbol{Q}^*$ (or equivalently $\boldsymbol{Q}^s$) by optimization technique GPSA. In view of Eq. (12), the λ is considered to be the real-numbered vector $\boldsymbol{x}$ (1-dimentional here) which is to be optimized in GPSA. Objective function f in GPSA is determined by MAPE between $\boldsymbol{Q}^{int}$ and $\boldsymbol{Q}^s$, and $f(\lambda)=\text{MAPE}$. The way to look for desirable $\boldsymbol{Q}^{int}$ is formulated as the following optimization problem.

$$\min_{\lambda} f(\lambda),\quad \text{s.t. } \frac{512}{255}\le\lambda\le 16 \tag{16}$$

Using GPSA, we can obtain the minimum MAPE in the search space of λ, and corresponding $\boldsymbol{Q}^{int}$ is our desirable integer quantization table. Having simulated in MATLAB, the minimum MAPE=1.03% is obtained when $\lambda=2.0517$ and then, with $\lambda=2.0517$, corresponding desirable $\boldsymbol{Q}^{int}$ shown in Fig. 8 is obtained, which is calculated by Eqs. (13) and (14).

4	6	7	8	10	13	18	31
6	9	10	12	15	20	28	48
7	10	12	14	18	23	32	55
8	12	14	17	21	27	38	65
10	15	18	21	26	33	47	80
13	20	23	27	33	43	61	103
18	28	32	38	47	61	86	146
31	48	55	65	80	103	146	250

Fig. 8. The proposed luminance quantization table $\boldsymbol{Q}^{int}$, which can be used directly in baseline JPEG without causing compatibility problems.

IV. Experimental Results and Comparisons with APBT-JPEG and DCT-JPEG

Before presenting the experimental results, it is worth discussing some experiment related issues. In order to test the proposed quantization table and compare it with other quantization tables, in this section, we will present simulation results obtained by applying different image compression algorithms to test typical monochrome images Barbara and Airplane (512×512, 8bpp). Airplane is smooth and flat. On the contrary, Barbara contains more details and edges. Throughout this paper, all experiments are conducted with MATLAB 7.14.

In APBT-JPEG, $\boldsymbol{V}$ (when N=8) is used as the transform matrix. In the quantization part, the uniform

quantization table (see Fig. 3(a)) is adopted, while in baseline DCT-JPEG algorithm, $\boldsymbol{C}$ is used in transform step with six different quantization tables used in quantization procedure respectively (see Fig. 3(b), Fig. 5, Fig. 8 and Fig. 9). Three baseline JPEG's optimized quantization tables (shown in Fig. 9) were proposed in other works which are chosen for comparison here. All of these JPEG algorithms use the typical Huffman tables (see [3]) which have been developed from the average statistics of a large set of images with 8-bit precision. For the sake of image compression performance assessment, the distortion is measured by the PSNR, which is the most widely used image quality metric:

$$\mathrm{PSNR} = 10\log_{10}\left(\frac{255^2}{\mathrm{MSE}}\right)(\mathrm{dB}) \tag{17}$$

where MSE denotes the mean squared error between the original and reconstructed images.

A. PSNR Comparison of APBT-JPEG, and DCT-JPEG with Different Quantization Tables

Table I and Table II show the experimental results with APBT-JPEG using uniform quantization table and DCT-JPEG using different quantization tables in terms of PSNR at different bit rates, applied to images Airplane and Barbara, respectively. In what follows, coding performance results is summarized on the basis of PSNR. In view of Table I and Table II, firstly, compared with APBT-JPEG, an identical coding performance could be achieved by using DCT-JPEG with quantization table $\boldsymbol{Q}^*$, and a very approximate coding performance could be achieved by using DCT-JPEG with proposed quantization table. Secondly, coding performance of DCT-JPEG using proposed quantization table outperforms DCT-JPEG using default quantization table and quantization table 1 at various bit rates. Thirdly, compared with DCT-JPEG using quantization table 2, coding performance of DCT-JPEG using proposed quantization table is better at low bit rates, but at other bit rates, coding performance of DCT-JPEG using proposed quantization table is worse. Lastly, compared with DCT-JPEG using quantization table 3, coding performance of DCT-JPEG using proposed quantization table is better at low bit rates, and is comparable at higher rates.

Furthermore, to keep the paper reasonably concise, we would like to point out that the identical experiment simulation is also applied to other test images, and similar objective quality assessment results are obtained.

B. Visual Quality Comparison of APBT-JPEG, and DCT-JPEG with Different Quantization Tables

PSNR is just a mathematical model that approximates results of subjective quality assessment. In order to compare the compression performance subjectively, Figs. 10~14 show the reconstructed images Barbara and Airplane obtained by using APBT-JPEG with uniform quantization table and DCT-JPEG with different quantization tables at some representative bit rates.

1	1	1	1	2	5	6	5
1	1	1	2	4	5	6	5
1	1	2	2	5	8	8	6
1	2	3	5	6	10	10	7
2	3	5	6	8	10	11	9
4	6	7	8	10	12	12	10
7	9	9	9	11	10	10	9
4	6	6	7	8	10	9	9

(a)

16	16	16	16	17	18	21	24
16	16	16	16	17	19	22	25
16	16	17	18	20	22	25	29
16	16	18	21	24	27	31	36
17	17	20	24	30	35	41	47
18	19	22	27	35	44	54	65
21	22	25	31	41	54	70	88
24	25	29	36	47	65	88	115

(b)

16	14	13	15	19	28	37	55
14	13	15	19	28	37	55	64
13	15	19	28	37	55	64	83
15	19	28	37	55	64	83	103
19	28	37	55	64	83	103	117
28	37	55	64	83	103	117	117
37	55	64	83	103	117	117	111
55	64	83	103	117	117	111	90

(c)

Fig. 9. (a) The quantization table for luminance (quantization table 1) employed by the JPEG encoder on the Apple iPhone 4/4S models [19], (b) The HVS-based luminance quantization table (quantization table 2) which is derived by incorporating the human visual system model with a uniform quantizer [20], (c) The luminance quantization table (quantization table 3) generated from psycho-visual error threshold for DCT basis functions, with having investigated a psycho-visual error threshold at DCT frequency on the grayscale image [21].

TABLE I: PSNR COMPARISON OF APBT-JPEG, AND DCT-JPEG USING DIFFERENT QUANTIZATION TABLES, APPLIED TO IMAGE AIRPLANE.

Bit rate (bpp)	**APBT-JPEG**	**DCT-JPEG**					
	Uniform quantization table [7]	Quantization table $\boldsymbol{Q}^*$	Proposed quantization table	Default quantization table	Quantization table 1 [19]	Quantization table 2 [20]	Quantization table 3 [21]
0.15	25.74	25.74	**25.76**	24.90	25.29	25.02	25.06
0.20	28.04	28.04	**28.09**	27.70	27.87	27.83	27.81
0.25	29.78	29.78	**29.79**	29.48	29.58	29.56	29.62
0.30	30.90	30.90	**30.92**	30.81	30.70	30.93	30.98
0.40	32.83	32.83	**32.86**	32.73	32.51	32.98	32.94
0.50	34.28	34.28	**34.31**	34.21	33.71	34.59	34.39
0.60	35.40	35.40	**35.41**	35.34	34.74	35.91	35.46
0.75	36.91	36.91	**36.92**	36.61	36.07	37.51	36.88
1.00	38.80	38.80	**38.80**	38.39	37.74	39.48	38.70
1.25	40.22	40.22	**40.22**	39.80	39.20	41.04	40.13
1.50	41.46	41.46	**41.45**	41.03	40.48	42.39	41.36

TABLE II: PSNR COMPARISON OF APBT-JPEG, AND DCT-JPEG USING DIFFERENT QUANTIZATION TABLES, APPLIED TO IMAGE BARBARA.

Bit rate (bpp)	APBT-JPEG	DCT-JPEG					
	Uniform quantization table [7]	Quantization table $\boldsymbol{Q}^*$	Proposed quantization table	Default quantization table	Quantization table 1 [19]	Quantization table 2 [20]	Quantization table 3 [21]
0.15	22.80	22.80	**22.79**	22.41	22.59	22.18	22.50
0.20	23.86	23.86	**23.87**	23.59	23.70	23.53	23.76
0.25	24.69	24.69	**24.69**	24.44	24.34	24.78	24.60
0.30	25.51	25.51	**25.51**	25.19	24.89	25.82	25.41
0.40	27.07	27.07	**27.07**	26.61	26.10	27.62	26.95
0.50	28.42	28.42	**28.41**	27.95	27.33	29.18	28.34
0.60	29.68	29.68	**29.68**	29.23	28.53	30.62	29.61
0.75	31.39	31.39	**31.39**	30.90	30.20	32.38	31.29
1.00	33.59	33.59	**33.59**	33.23	32.57	34.75	33.56
1.25	35.38	35.38	**35.38**	35.10	34.52	36.64	35.40
1.50	36.83	36.83	**36.83**	36.71	36.15	38.20	36.94

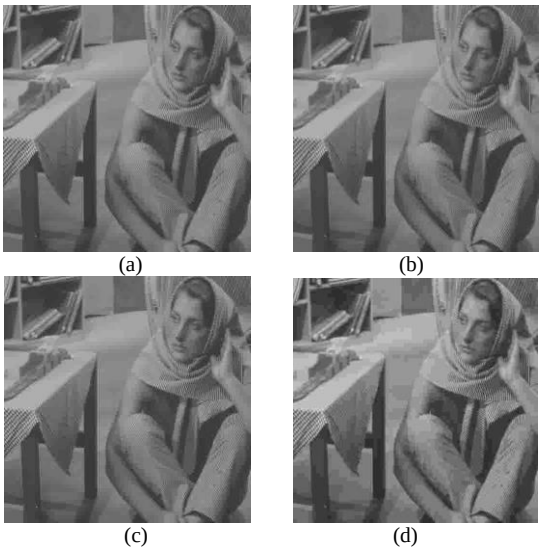

(a) (b) (c) (d)

Fig. 10. Barbara obtained at 0.20bpp: (a) APBT-JPEG version using uniform quantization table, with PSNR=23.86dB, (b) DCT-JPEG version using quantization table $\boldsymbol{Q}^*$, with PSNR=23.86dB, (c) DCT-JPEG version using proposed quantization table, with PSNR=23.87dB, (d) DCT-JPEG version using default quantization table, with PSNR=23.59dB.

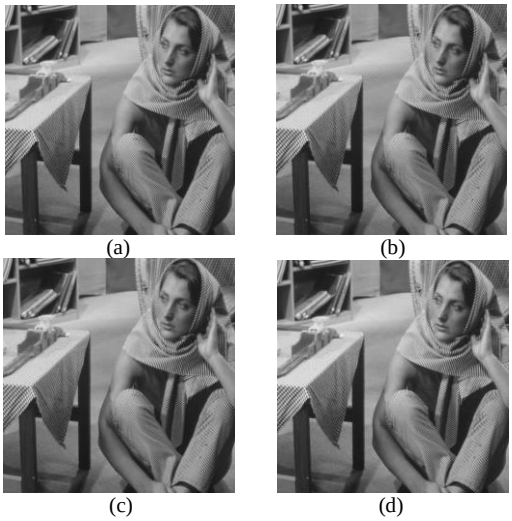

(a) (b) (c) (d)

Fig. 11. Barbara obtained at 1.00bpp: (a) APBT-JPEG version using uniform quantization table, with PSNR=33.59dB, (b) DCT-JPEG version using quantization table $\boldsymbol{Q}^*$, with PSNR=33.59dB, (c) DCT-JPEG version using proposed quantization table, with PSNR=33.59dB, (d) DCT-JPEG version using default quantization table, with PSNR=33.23dB.

From Fig. 10 (at 0.20bpp) and Fig. 11 (at 1.00bpp), as compared with APBT-JPEG, a very approximate visual quality of reconstructed image Barbara is achieved by using DCT-JPEG with quantization table $\boldsymbol{Q}^*$ and proposed quantization table. In Fig. 10, at bit rate 0.20bpp, since the blocking artifacts have been reduced significantly, reconstructed images of DCT-JPEG using proposed quantization table look more agreeable than DCT-JPEG version using default quantization table. With bit rate increasing, the reconstructed images of these JPEG algorithms are visually closer to the original one. In Fig. 11, at bit rate 1.00bpp, unlike the PSNR difference between images Barbara reconstructed by DCT-JPEG with proposed quantization table and default quantization table, the visual difference between them is almost visually imperceptible.

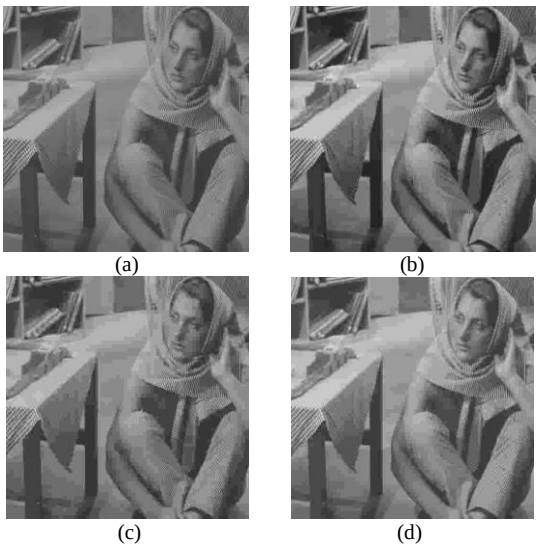

(a) (b) (c) (d)

Fig. 12. Barbara obtained at 0.20bpp: (a) DCT-JPEG version using proposed quantization table, with PSNR=23.87dB, (b) DCT-JPEG version using quantization table 1, with PSNR=23.70dB, (c) DCT-JPEG version using quantization table 2, with PSNR=23.53dB, (d) DCT-JPEG version using quantization table 3, with PSNR=23.76dB.

As shown in Fig. 12 (at 0.20bpp), since the blocking artifacts have been reduced significantly, DCT-JPEG using proposed quantization table yields more visually pleasant results, while DCT-JPEG versions using quantization table 1, 2 and 3 suffer from discontinuities

across block boundaries. In Fig. 13 (at 1.00bpp), the visual difference among images Barbara reconstructed by DCT-JPEG with proposed quantization table and quantization table 1, 2 and 3 is almost visually imperceptible.

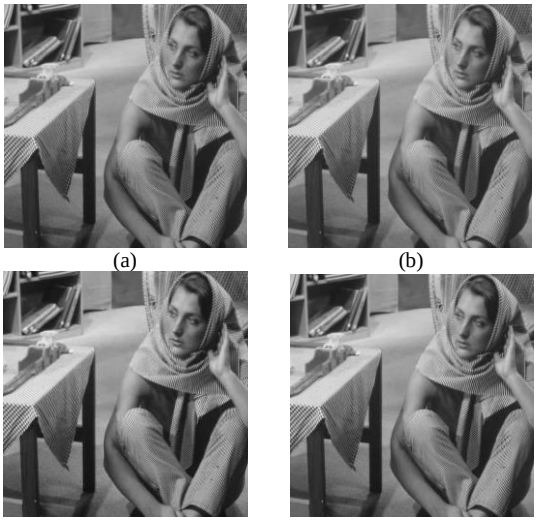

Fig. 13. Barbara obtained at 1.00bpp: (a) DCT-JPEG version using proposed quantization table, with PSNR=33.59dB, (b) DCT-JPEG version using quantization table 1, with PSNR=32.57dB, (c) DCT-JPEG version using quantization table 2, with PSNR=34.75dB, (d) DCT-JPEG version using quantization table 3, with PSNR=33.56dB.

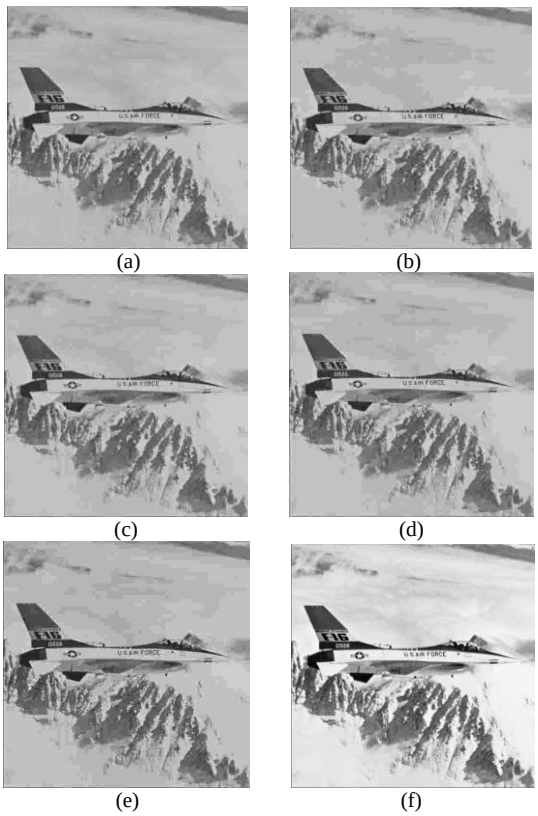

Fig. 14. Airplane obtained at 0.20bpp: (a) DCT-JPEG version using proposed quantization table, with PSNR=28.09dB, (b) DCT-JPEG version using default quantization table, with PSNR=27.70dB, (c) DCT-JPEG version using quantization table 1, with PSNR=27.87dB, (d) DCT-JPEG version using quantization table 2, with PSNR=27.83dB, (e) DCT-JPEG version using quantization table 3, with PSNR=27.81dB. (f) Original image "Airplane".

As described earlier, actually, the advantage of DCT-JPEG with proposed quantization table is the less visibility of blocking artifacts in reconstructed images at low bit rates. Then, similar result is obtained when experiment simulation is applied to image Airplane. As shown in Fig. 14, compared with DCT-JPEG versions using default quantization table, quantization table 1, 2 and 3, better visual quality of DCT-JPEG version using proposed quantization table is achieved at low bit rates, and the blocking artifacts have also been reduced significantly.

To keep the paper reasonably concise, finally, we would like to point out that similar subjective quality assessment results are obtained, when the identical experiment simulation is applied to other test images.

In short, among these image compression algorithms, the image reconstructed by DCT-JPEG using proposed quantization table is always good at various bit rates in the sense of subjective visual quality.

V. Conclusions

This paper has proposed a novel luminance quantization table used in baseline JPEG. Tested by natural images, we can see that compared with DCT-JPEG using other quantization tables, the proposed quantization table improves the performance of baseline JPEG at low bit rates, both in terms of PSNR and visual quality. Due to its superiority in reducing the blocking artifacts of reconstructed image at low bit rates, we call it deblocking quantization table. Especially, employing deblocking quantization table instead of default one in baseline JPEG, reconstructed image has better performance at various bit rates. Thus, deblocking quantization table is a good alternative of widely used default quantization table suggested by JPEG.

Interestingly, deblocking quantization table can be adopted both as luminance and chrominance quantization table in DCT-JPEG for color image compression and an almost the same coding performance would be achieved compared with APBT-JPEG. With using deblocking quantization table, we also can achieve the almost identical coding performance by replacing APBT with DCT in SA-APBT (or D-APBT) algorithm. Furthermore, we can continue to explore other applications of the deblocking quantization table, such as MPEG-4 video coding. Therefore, we can foresee that the proposed quantization table will be widely used in the field of image compression.

Acknowledgment

This work was supported by the National Natural Science Foundation of China (Grant No. 61201371) and the promotive research fund for excellent young and middle-aged scientists of Shandong Province, China (Grant No. BS2013DX022). The authors would like to thank Fanfan Yang, Liping Wang, and Heng Zhang for their kind help and valuable suggestions. The authors

would like to thank the anonymous reviewers and the editor for their valuable comments to improve the presentation of the paper.

REFERENCES

[1] A. Skodras, C. Christopoulos, and T. Ebrahimi, "The JPEG 2000 still image compression standard," *IEEE Signal Processing Magazine*, vol. 18, no. 5, pp. 36-58, Sep. 2001.

[2] F. Dufaux, G. J. Sullivan, and T. Ebrahimi, "The JPEG XR image coding standard," *IEEE Signal Processing Magazine*, vol. 26, no. 6, pp. 195-199, 204, Nov. 2009.

[3] G. K. Wallace, "The JPEG still picture compression standard," *Communications of the ACM*, vol. 34, no. 4, pp. 30-44, Apr. 1991.

[4] A. Beghdadi, M. C. Larabi, A. Bouzerdoum, and K. M. Iftekharuddin, "A survey of perceptual image processing methods," *Signal Processing: Image Communication*, vol. 28, no. 8, pp. 811-831, Sep. 2013.

[5] J. Kim and C. B. Sim, "Compression artifacts removal by signal adaptive weighted sum technique," *IEEE Trans. on Consumer Electronics*, vol. 57, no. 4, pp. 1944-1952, Nov. 2011.

[6] S. A. Golestaneh and D. M. Chandler, "Algorithm for JPEG artifact reduction via local edge regeneration," *Journal of Electronic Imaging*, vol. 23, no. 1, pp. 14, Jan. 2014.

[7] Z. X. Hou, C. Y. Wang, and A. P. Yang, "All phase biorthogonal transform and its application in JPEG-like image compression," *Signal Processing: Image Communication*, vol. 24, no. 10, pp. 791-802, Nov. 2009.

[8] Z. X. Hou, Z. H. Wang, and X. Yang, "Design and implementation of all phase DFT digital filter," *Acta Electronica Sinica*, vol. 31, no. 4, pp. 539-543, Apr. 2003.

[9] C. Y. Wang, B. C. Jiang, and S. Z. Xie, "Properties of all phase biorthogonal transform matrix and its application in color image compression," *Journal of Computational Information Systems*, vol. 9, no. 18, pp. 7227-7234, Sep. 2013.

[10] C. X. Zhang, C. Y. Wang, and B. C. Jiang, "Color image compression based on directional all phase biorthogonal transform," *International Journal of Multimedia and Ubiquitous Engineering*, vol. 10, no. 1, pp. 247-254, Jan. 2015.

[11] B. C. Jiang, A. P. Yang, C. Y. Wang, and Z. X. Hou, "Shape adaptive all phase biorthogonal transform and its application in image coding," *Journal of Communications*, vol. 8, no. 5, pp. 330-336, May 2013.

[12] X. Y. Wang, B. C. Jiang, C. Y. Wang, Z. Q. Yang, and C. X. Zhang, "All phase biorthogonal transform and its application in MPEG-4 video compression," *International Journal of Signal Processing, Image Processing and Pattern Recognition*, vol. 7, no. 4, pp. 13-22, Aug. 2014.

[13] C. W. Kok, "Fast algorithm for computing discrete cosine transform," *IEEE Trans. on Signal Processing*, vol. 45, no. 3, pp. 757-760, Mar. 1997.

[14] J. Liang and T. D. Tran, "Fast multiplierless approximations of the DCT with the lifting scheme," *IEEE Trans. on Signal Processing*, vol. 49, no. 12, pp. 3032-3044, Dec. 2001.

[15] K. Lengwehasatit and A. Ortega, "Scalable variable complexity approximate forward DCT," *IEEE Trans. on Circuits and Systems for Video Technology*, vol. 14, no. 11, pp. 1236-1248, Nov. 2004.

[16] W. M. Li, Z. H. Jiang, T. L. Wang, and H. P. Zhu, "Optimization method based on generalized pattern search algorithm to identify bridge parameters indirectly by a passing vehicle," *Journal of Sound and Vibration*, vol. 333, no. 2, pp. 364-380, Jan. 2014.

[17] R. M. Lewis, A. Shepherd, and V. Torczon, "Implementing generating set search methods for linearly constrained minimization," *SIAM Journal on Scientific Computing*, vol. 29, no. 6, pp. 2507-2530, Oct. 2007.

[18] C. Audet and J. E. Dennis, "Pattern search algorithms for mixed variable programming," *SIAM Journal on Optimization*, vol. 11, no. 3, pp. 573-594, Mar. 2000.

[19] C. Sun and E. H. Yang, "An efficient DCT-based image compression system based on Laplacian transparent composite model," *IEEE Trans. on Image Processing*, vol. 24, no. 3, pp. 886-900, Mar. 2015.

[20] C. Y. Wang, S. M. Lee, and L. W. Chang, "Designing JPEG quantization tables based on human visual system," *Signal Processing: Image Communication*, vol. 16, no. 5, pp. 501-506, Jan. 2001.

[21] N. A. Abu, F. Ernawan, and N. Suryana, "A generic psychovisual error threshold for the quantization table generation on JPEG image compression," in *Proc. IEEE 9th International Colloquium on Signal Processing and Its Applications*, Kuala Lumpur, Malaysia, Mar. 8-10, 2013, pp. 39-43.

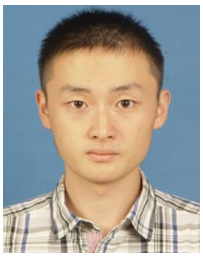

Qiming Fu was born in Jiangxi province, China in 1992. He received his B.S. degree in electronic information science and technology from Shandong University, Weihai, China in 2013. He is currently pursuing his M.E. degree in electronics and communication engineering at Shandong University, China. His current research interests include digital image processing and analysis techniques.

Baochen Jiang was born in Shandong province, China in 1962. He received his B.S. degree in radio electronics from Shandong University, China in 1983 and his M.E. degree in communication and electronic systems from Tsinghua University, China in 1990. Now he is a professor in the School of Mechanical, Electrical and Information Engineering, Shandong University, Weihai, China. His current research interests include signal and information processing, image/video processing and analysis, and smart grid technology.

Chengyou Wang was born in Shandong province, China in 1979. He received his B.E. degree in electronic information science and technology from Yantai University, China in 2004, and his M.E. and Ph.D. degree in signal and information processing from Tianjin University, China in 2007 and 2010 respectively. Now he is an associate professor and supervisor of postgraduate in the School of Mechanical, Electrical and Information Engineering, Shandong University, Weihai, China. His current research interests include digital image/video processing and analysis, multidimensional signal and information processing.

Xiao Zhou was born in Shandong province, China in 1982. She received her B.E. degree in automation from Nanjing University of Posts and Telecommunications, China in 2003, her M.E. degree in information and communication engineering from Inha University, Korea in 2005, and her Ph.D. degree in information and communication engineering from Tsinghua University, China in 2013. Now she is a lecturer in the School of Mechanical, Electrical and Information Engineering, Shandong University, Weihai, China. Her current research interests include wireless communication technology, digital image processing and analysis.